*The AAPS Journal (2020) 22: 88*
DOI: 10.1208/s12248-020-00467-8

*Research Article*

# Nano-delivery of Gemcitabine Derivative as a Therapeutic Strategy in a Desmoplastic KRAS Mutant Pancreatic Cancer

**Manisit Das,[1] Jun Li,[2,3] Michelle Bao,[1,4,5] and Leaf Huang[1,6]**

*Received 13 March 2020; accepted 22 May 2020; published online 22 June 2020*

***Abstract.*** Pancreatic ductal adenocarcinoma remains one of the challenging malignancies to treat, and chemotherapy is the primary treatment strategy available to most patients. Gemcitabine, one of the oldest chemotherapeutic drugs approved for pancreatic cancer, has limited efficacy, due to low drug distribution to the tumor and chemoresistance following therapy. In this study, we delivered gemcitabine monophosphate using lipid calcium phosphate nanoparticles, to desmoplastic pancreatic tumors. Monophosphorylation is a critical, rate-limiting step following cellular uptake of gemcitabine and precursor of the pharmacologically active gemcitabine triphosphate. Our drug delivery strategy enabled us to achieve robust tumor regression with a low parenteral dose in a clinically relevant, KRAS mutant, syngeneic orthotopic allograft, lentivirus-transfected KPC cell line-derived model of pancreatic cancer. Treatment with gemcitabine monophosphate significantly increased apoptosis of cancer cells, enabled reduction in the proportion of immunosuppressive tumor-associated macrophages and myeloid-derived suppressor cells, and did not increase expression of cancer stem cell markers. Overall, we could trigger a strong antitumor response in a treatment refractory PDAC model, while bypassing critical hallmarks of gemcitabine chemoresistance.

**KEY WORDS:** drug delivery; pancreatic cancer; chemotherapy; gemcitabine; nanoparticle.

## INTRODUCTION

Pancreatic cancer resulted in approximately 45,750 deaths and contributed to 56,770 new incidents of the disease in the USA in 2019 (1). The disease remains lethal, with 5-year survival rates ranging at around 9%. Cytotoxic chemotherapy is still regarded as a primary treatment strategy for most patients, with limited benefits. These approaches provide median survival benefit somewhere between 6 and 18 months in patients with advanced and metastatic malignancies (2,3). Surgery is considered the first-line treatment for patients with resectable tumors. For nonresectable borderline or locally advanced tumors, and metastatic tumors, chemotherapy such as FOLFIRINOX or gemcitabine remains the first-line treatment for patients with Eastern Cooperative Oncology Group (ECOG) performance status score ranging between 0 and 2. The best supportive care remains the only resort for patients with higher ECOG scores (4).

Cytotoxic nucleoside analogues are a prominent class of anticancer and antiviral small molecule drugs (5). Gemcitabine (2′,2′-difluoro-2′-deoxycytidine), one of the major nucleoside analog chemotherapeutics, is a standard intervention in pancreatic cancer. However, benefit is limited due to challenges of drug penetration in highly vascularized, desmoplastic tumors, and acquired chemoresistance in pancreatic cancer cells (6). Stand-alone gemcitabine treatment has limited benefit in patients with pancreatic cancer. These compounds serve as antimetabolites by interfering with nucleic acid synthesis and enzymes facilitating metabolism of nucleic acids (7). Locally advanced or metastatic pancreatic cancer patients were observed to have median survival of 32 weeks, with a progression-free survival of 13.5 weeks and an overall response rate of 13%, under gemcitabine monotherapy (8).

Gemcitabine is reliant on nucleoside transporters to enter cells and phosphorylated by deoxycytidine kinase (dCK), pyrimidine nucleoside monophosphate kinase, and potentially nucleoside diphosphate kinase sequentially to form mono-, di-, and triphosphate gemcitabine derivatives (6). The incorporation of the first phosphate group to form

[1] Division of Pharmacoengineering and Molecular Pharmaceutics, and Center for Nanotechnology in Drug Delivery, Eshelman School of Pharmacy, University of North Carolina at Chapel Hill, Chapel Hill, North Carolina 27599, USA.
[2] Qualiber Inc., Durham, North Carolina 27705, USA.
[3] *Present Address:* ZY Therapeutics, Research Triangle Park, North Carolina 27709, USA.
[4] North Carolina School of Science and Mathematics, Durham, North Carolina 27705, USA.
[5] *Present Address:* Stanford University, Stanford, California, USA.
[6] To whom correspondence should be addressed. (e–mail: leafh@email.unc.edu)

gemcitabine monophosphate is the rate-limiting step for subsequent phosphorylation to the triphosphate form and activation of gemcitabine (9,10). The triphosphate derivative incorporates into the DNA strand, rendering inhibition of replication by termination of DNA chain elongation (11). However, gemcitabine can be inactivated by rapid metabolism to 2′,2′-difluorodeoxyuridine mediated by the enzyme deoxycytidine deaminase, followed by renal excretion, when injected parenterally (12).

Using nanoparticle-based formulation systems and lipophilic prodrugs of gemcitabine had been some common approaches to bypass gemcitabine resistance, to circumvent the hurdle of nucleoside transport and deaminase-mediated inactivation (13,14), and to deliver combination therapies (15,16). However, post-cellular uptake, dCK, and other intracellular kinases are still required for conversion to triphosphate gemcitabine derivative.

To augment the therapeutic efficacy of gemcitabine by circumventing the delivery hurdles to desmoplastic pancreatic tumors, we encapsulated gemcitabine monophosphate (GMP), further bypassing the rate-limiting dCK mediated by conversion of gemcitabine into lipid calcium phosphate (LCP) nanoparticles (17,18). LCPs can protect drugs like GMP from enzymatic decomposition, bypass inactivation in blood circulation, and rapid renal elimination (19–21). Phosphorylated drugs such as GMP can be co-precipitated into the calcium phosphate core of LCP nanoparticles, which we have shown to be capable of accumulating in desmoplastic pancreatic tumors (22).

LCP nanoparticles enable encapsulation of a wide range of phosphorylated drugs (23). Here, we investigated the efficacy of a GMP nanoformulation (Nano GMP) in mounting an antitumor response in an orthotopic syngeneic allograft KPC model of pancreatic cancer. KPC, a genetically engineered mouse model, with oncogenic driver mutations in KRAS and p53, is a clinically relevant model of pancreatic ductal adenocarcinoma (PDAC) (24–26). We hypothesized that formulation of monophosphorylated gemcitabine in LCP nanoparticles will enable enrichment of the drug in desmoplastic pancreatic tumor tissues and enable a robust tumor regression benefit. We were subsequently interested in alterations to the immune tumor microenvironment (TME) post-administration of Nano GMP. PDAC tumors in both humans and KPC mice manifest intricate networks of immunosuppressive tumor-infiltrating leukocytes, and dense desmoplastic stroma, setting steep challenges for most therapeutic interventions. The resistance of pancreatic cancer to immunotherapy limits long-term antitumor response and is usually accounted for by defective T cells, desmoplastic barriers to T cell infiltration, immunosuppressive tumor microenvironment (TME), and low mutational burden (27). We wanted to explore if the combination of GMP nanoformulation with immune adjuvant therapy can enable a synergistic antitumor response. We aimed at analyzing the effect on tumor growth and downstream effect on tumor infiltrates when Nano GMP was combined with 5′ triphosphate double-stranded RNA (ppp dsRNA), a pathogen-associated molecular pattern (PAMP) capable of actuating inflammatory innate immune response (22). We delivered both GMP and ppp dsRNA, two unique phosphorylated drugs, using LCP nanoparticles.

## MATERIALS AND METHODS

### Materials

N-(Methylpolyoxyethylene oxycarbonyl)-1,2-distearoyl-sn-glycero-3-phosphoethanolamine, sodium salt (DSPE-PEG 2000, PEG chain molecular weight, 2000), and 1,2-dioleoyl-3-trimethylammonium-propane chloride salt (DOTAP) were procured from NOF Corporation (Tokyo, Japan). Cholesterol was sourced from Sigma-Aldrich (St. Louis, MO, USA). GMP disodium salt was procured from HDH Pharma (Morrisville, NC, USA). Matrigel matrix for tumor inoculation was obtained from Corning (NY, USA). Antibodies for flow cytometry were procured from BioLegend and eBioscience (San Diego, CA, USA). Prolong Gold Antifade Reagent with DAPI was supplied by Life Technologies Corporation (Carlsbad, CA, USA). DeadEnd™ Fluorometric TUNEL System was obtained from Promega (Madison, WI, USA). 5′ triphosphate double-stranded RNA (tlrl-3prna, 5'ppp-dsRNA) was purchased from InvivoGen (San Diego, CA, USA). FITC Annexin V Apoptosis Detection Kit I was obtained from BD Biosciences (San Jose, CA, USA). XenoLight D-Luciferin - K+ Salt Bioluminescent Substrate was procured from PerkinElmer (Waltham, MA, USA).

### Statistical Analyses

We reported data as mean ± standard error of mean (SEM), and replicates for each experiment as "n." GraphPad Prism was used for statistical analyses. Student's *t* test was used for comparing two sets of values, and ordinary one-way-analysis-of-variance (ANOVA) for three sets of values and above, with Tukey's or two-stage linear step-up procedure of Benjamini, Krieger, and Yekutieli multiple comparisons test for pairwise comparisons. *, **, ***, and **** designates $p < 0.05$, 0.01, 0.001, and 0.0001.

### Cell Lines

Primary tumor cell lines of pancreatic ductal adenocarcinoma were derived from a genetically engineered mouse model (LSL-Kras G12D/+; LSL-Trp53R172H/+; Pdx-1-Cre, syngeneic to C57BL/6 strain) and obtained as a generous gift from Dr. Serguei Kozlov from Center for Advanced Preclinical Research, Frederick National Laboratory for Cancer Research (NCI). Cells were cultured in Dulbecco's Modified Eagle Medium: Nutrient Mixture F-12 (DMEM/F12) and supplemented with fetal bovine serum (FBS, 10%) (Gibco), Penicillin/Streptomycin (1%) at 37 °C, and 5% CO2 in a humidified atmosphere. The primary cell lines were stably transfected with lentiviral vector carrying mCherry red fluorescent protein (RFP) and firefly luciferase (Luc). The stably transfected cell lines (KPCF1) were used for *in vivo* studies and monitored by bioluminescence.

### Orthotopic Pancreatic Tumor Model

All animal experiments were conducted in compliance with regulations of the University of North Carolina at

Chapel Hill Institutional Animal Care and Use Committee (IACUC). Orthotopic pancreatic tumors were inoculated as previously described (22). Sub-Confluent KPCF1 cells were trypsinized, washed in ice-cold PBS, and resuspended in 1:1 mixture of Matrigel Matrix (Corning): phosphate-buffered saline (PBS). The cells were injected in the pancreas of 8–10-week-old C57BL/6 mice anesthetized with isoflurane ($10^6$ cells per mice in a volume of 50 μL). USP grade Meloxicam (Thomas Scientific) was administered as a post-operative analgesic.

### Bioluminescence Imaging to Monitor Tumor Growth

Tumor growth was monitored by bioluminescence imaging using an IVIS Lumina Series III *In vivo* imaging system (PerkinElmer). Anesthetized animals were administered D-luciferin (100 mg/kg of body weight), intraperitoneally, and bioluminescence was recorded 5 min past administration. Bioluminescence signal intensity was reported as radiance, a measurement of photons emitted from the subject, in the units of photons/s/cm$^2$/sr. The radiance values were log-normalized and tabulated.

### Nanoparticle Formulation of Gemcitabine Monophosphate

Three hundred μL of calcium chloride ($CaCl_2$) (5 M) was mixed with 300 μL of gemcitabine monophosphate (GMP) (60 mM) in 20 mL of cyclohexane: Igepal CO-520 (79/21 *v*/v) oil phase. Likewise, 600 μL of 200-mM diammonium phosphate [$(NH_4)_2HPO_4$] was added to 20 mL of cyclohexane/Igepol (V/V: 79/21). The phosphate and calcium emulsions were mixed with each other, after individually stirring for 5 min. After another 5 min, 400 μL of dioleoylphosphatidic acid (DOPA) (20 mg/mL) was added to the combined emulsion. The reaction was stirred for 20 min, which was followed by addition of 40 mL of 200 proof ethanol, and further stirring for 5 min. The disrupted microemulsion was centrifuged at 10,000xg for 15 min. The particles are washed again with 200-proof ethanol, at 10,000xg for 10 min, and the supernatant was discarded. The precipitate was dissolved in 2 mL of dichloromethane (DCM). The DCM solution was centrifuged at 10,000xg for 5 min, and the clear DCM supernatant was collected and stored in − 20 °C until further use. To the DCM solution of the core particles, 400 μL of DOTAP (20 mM in DCM), 400 μL of cholesterol (20 mM in DCM), and 240 μL of DSPE-PEG (20 mM in DCM) were added. The DCM was evaporated to form a thin film, and minimal volume of ethanol was added to suspend the lipid film, with brief sonication. The resultant clear solution was added into 2000 μL of deionized (DI) water. One hundred milligrams of sucrose was added to the solution and subsequently passed through a 0.45-μm filter. The formulation was transferred into 20-mL serum vials and lyophilized for subsequent storage in 4 °C until use. The lyophilized formulation was rehydrated using DI water prior administration. The final lyophilized nanoformulation containing the calcium phosphate and lipids has a mass of 10 mg per dose of GMP (1.16 μmole/mouse or 0.45 mg/mouse).

### Nanoparticle Formulation of 5′ Triphosphate Double-Stranded RNA

LCP nanoparticles encapsulating 5′ triphosphate double-stranded RNA (ppp dsRNA) were prepared using a protocol as described previously (28), with additional modifications. Briefly, ppp dsRNA (200 μg, 0.25 mg/mL) solution was mixed with $CaCl_2$ (2.5 M, 1800 μL). An $(NH4)_2HPO_4$ solution (1800 μL, 50 mM) was independently prepared. The calcium and phosphate solutions were separately added to stirring oil phases prepared with Igepal CO-520 and cyclohexane (3:7 v/v) to drive the formation of calcium phosphate nanoprecipitates. The microemulsion was stirred for 5 min before addition of DOPA (20 mM in chloroform/dichloromethane (DCM), 1400 μL) and stirred further for 30 min. The microemulsion was disrupted by 200-proof ethanol, centrifuged at 10,000xg for 20 min, and further washed with 200-proof ethanol to remove trace Igepal, cyclohexane, and un-encapsulated dsRNA. The precipitate was finally suspended in 10 mL of dichloromethane and centrifuged at 14,000 RPM for 5 min to ensure removal of large aggregates. These "core" nanoparticles were determined to encapsulate approximately 70% of the input ppp dsRNA (14-μg ppp dsRNA/mL of DCM). The final particles for therapeutic administration were prepared by adding 357 μL of the "core" LCP, as synthesized in the previous steps to 80 μL of DOTAP (36 mM in DCM), 145 μL of cholesterol, (20 mM in DCM), 128 μL of DSPE-PEG (20 mM in DCM). The lipid film was formed by removal of dichloromethane under nitrogen gas flow, followed by resuspension in 5% glucose solution and sonication before intravenous administration.

### Physicochemical Characterization of Nanoparticles

Particle sizes of LCP were analyzed by a Malvern ZetaSizer (Westborough, MA). Transmission electron microscope (TEM) images of the calcium phosphate core particles were captured via a JEOL 100CX II microscope (JEOL, Japan). About 5 μL of samples was placed on a 300-mesh carbon coated copper grid procured from Ted Pella, Inc., in Redding, CA. Prior to TEM imaging, 1% uranyl acetate solution was used for negative staining the nanoparticles for 5 min.

### Characterization of Tumor-Infiltrating Immune Cells Using Flow Cytometry

Post-sacrifice, orthotopic pancreatic tumors were harvested and enzymatically digested with Type IV Collagenase (Gibco) and deoxyribonuclease I (Alfa Aesar). The samples were subsequently passed through 40-μm cell strainer (Corning), washed with and resuspended in fluorescence-activated cell sorting (FACS) buffer (PBS supplemented with 10% fetal bovine serum (FBS), and 2-mM ethylenediaminetetraacetic acid {EDTA}). Cells were stained with fluorescent-conjugated antibodies, and fluorescence parameters were recorded with Becton Dickinson LSR II (HTS) flow cytometry analyzer. End-stage apoptotic and necrotic cells were stained by fluorescein isothiocyanate (FITC) Annexin V Apoptosis Detection Kit I and marked by FITC Annexin V

and Propidium Iodide positive cells. OneComp eBeads™ Compensation Beads (ThermoFisher Scientific) were used for single-color compensation controls. Data were analyzed using FlowJo V10.

### Immunofluorescence Staining

Tumor tissues were harvested from animals sacrificed post-treatment, rinsed in PBS, and incubated with 4% paraformaldehyde (PFA) at 4 °C for 48 h. Following fixation, tissues were placed in 30% sucrose overnight at 4 °C for cryoprotection. Tissues were embedded in OCT compound (Fisher Scientific, Pittsburgh, PA) and sectioned by a microtome cryostat (H/I Hacker Instruments & Industries, Winnsboro, SC). TUNEL assays were conducted using the DeadEnd Fluorometric TUNEL System (Promega, Madison, WI) as per manufacturer's instructions. Cell nuclei staining positive for fluorescein-12-dUTP (green) were designated as TUNEL positive nuclei. Specimens were counterstained with DAPI, and Olympus BX61 microscope was used to image samples and analyzed by ImageJ software.

## RESULTS

### Nanoformulation of Gemcitabine Monophosphate Enables Tumor Regression in Orthotopic KPC Cell Line-Derived Model of Pancreatic Cancer

We outlined the schematic of the *in vivo* delivery of GMP via LCP nanoparticles on Fig. 1a. The physicochemical characterizations of the nanoparticles are presented on Fig. 1b and c. Our results showed that in the orthotopic KPC model of pancreatic cancer, while free gemcitabine was incapable of providing a significant tumor regression benefit, we observed a significant reduction in tumor burden post-single administration of GMP nanoformulation (Fig. 2a). The tumor burden reduced from $1.78 \pm 0.17$ g in the phosphate-buffered saline (PBS)-treated group to $0.90 \pm 0.17$ g in the Nano GMP group ($p < 0.01$), when monitored 7 days after the single therapeutic dose. The tumor regression benefit was also evident on a shorter time scale. When we administered the Nano GMP following a modified regimen and sacrificed the animals 1 day after the final dose, we saw a similar trend in antitumor response as we saw earlier (Fig. 2b). The tumor burden decreased from $1.62 \pm 0.29$ g in PBS group to $0.86 \pm 0.17$ g in the Nano GMP group ($p < 0.05$).

We further explored if the Nano GMP can achieve tumor regression in advanced pancreatic tumors. We chose to monitor the tumor growth via both bioluminescence and tumor burden measurement post-therapy (Fig. 2c–d). Our KPC cell line was transfected with luciferase allowing us to use bioluminescent signal intensity as a parameter to quantify cancer cells in the tumor. Treatment was initiated when signal intensity of $5 \times 10^7$ photons/s/cm$^2$/sr was attained. At the end of the treatment, tumor signal in the PBS group increased to $8.94 \pm 0.69$-fold relative to the baseline while those in the Nano GMP reduced to $0.33 \pm 0.13$-fold relative to baseline tumor signal (Fig. 2c), with a significant difference in mean fold-change ($p < 0.0001$). When we measured the absolute tumor burden at sacrifice (Fig. 2d), a significant difference ($p < 0.01$) was observed between PBS ($2.73 \pm 0.11$ g) and Nano GMP ($1.64 \pm 0.17$ g).

### Nanoparticle-Mediated Delivery of Gemcitabine Monophosphate Enhances Apoptosis in Pancreatic Tumor

We investigated if Nano GMP would induce apoptosis in the KPC tumors. We measured apoptosis by terminal deoxynucleotidyl transferase dUTP nick end labeling (TUNEL) staining through immunofluorescence, and Annexin V-Propidium iodide (PI) labeling through flow cytometry (Fig. 3). We found a significant ($p < 0.01$) increase in the expression of TUNEL positive area (green) in the microscopic field of view from PBS ($0.24 \pm 0.07\%$) to Nano GMP ($3.21 \pm 0.60\%$) group (Fig. 3a–b). We did not see a strong alignment of red fluorescent protein (RFP) positive cancer cells (red) with TUNEL-positive cells (green). It is possible apoptotic cells include fibroblast and immune cells. When we assayed end-stage apoptotic and necrotic cells using Annexin $V^+$ $PI^+$ staining by flow cytometry (Fig. 3c), the percentage of cells staining doubly positive increased significantly ($p < 0.01$) from PBS ($16.58 \pm 1.69\%$) to Nano GMP ($24.38 \pm 1.19\%$).

### Effect of Gemcitabine Monophosphate Nanoformulation on Tumor-Infiltrating Immune Cells

We assayed the changes in the proportion of immune infiltrates in the KPC tumor by flow cytometry (Fig. 4). No significant changes were observed in the population of T cells, ratio of cytotoxic T lymphocytes and regulatory T (Treg) cells, activated dendritic cells (DC), cancer stem cells, and PD-L1 positive cells. A significant difference ($p < 0.05$) in $CD11b^+$ $Gr\text{-}1^+$ myeloid-derived suppressor cells (MDSCs) was observed between the PBS ($4.31 \pm 0.88\%$) and Nano GMP ($2.52 \pm 0.27\%$) group. A statistically significant decrease ($p < 0.01$) of M2 macrophages was observed in the Nano GMP group ($1.99 \pm 0.22\%$) *vs.* PBS group ($0.86 \pm 0.15\%$) as well.

### Combination of Gemcitabine Monophosphate Nanoformulation Chemotherapy and Adjuvant Immune Therapy Can Reprogram Tumor Immune Microenvironment

To explore if combination with adjuvant immune therapy will enable TME modulation and induce a synergistic antitumor response, we combined Nano GMP with RIG-I agonist 5′-triphosphate double-stranded RNA (ppp dsRNA). The ppp dsRNA was formulated in LCP nanoparticles. We observed a sequence dependence on the antitumor effect observed with the combination of Nano GMP and ppp dsRNA LCP. When Nano GMP was injected before ppp dsRNA LCP (Fig. 5a), a significant reduction in tumor burden at sacrifice was observed for both Nano GMP ($0.90 \pm 0.17$ g) and Nano GMP and ppp dsRNA LCP combination ($1.07 \pm 0.13$ g), compared with the PBS-treated group ($1.78 \pm 0.17$ g). No statistically significant difference was observed between Nano GMP alone, or in combination with ppp dsRNA LCP. When we administered an alternate treatment regimen where ppp dsRNA LCP was administered before Nano GMP, no significant regression in tumor burden was

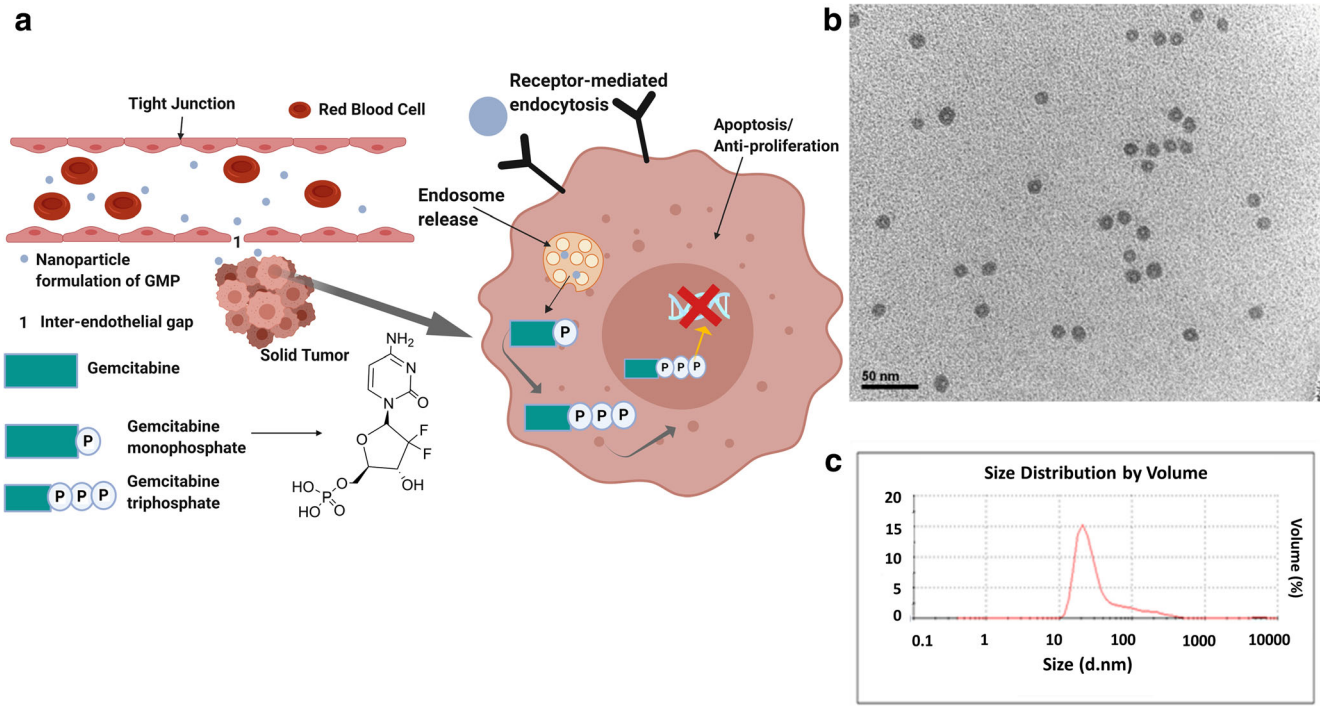


**Fig. 1.** Delivery of Gemcitabine monophosphate nanoformulation (Nano GMP) to cancer cells *in vivo,* **a** Schematic illustration of the delivery mechanism of Nano GMP, **b** transmission electron microscopy (TEM) image of Nano GMP, **c** hydrodynamic size distribution of Nano GMP measured by dynamic light scattering

observed with Nano GMP mono- or combination therapy, relative to PBS (Fig. 5b).

We assayed the changes in tumor-infiltrating immune cells in the KPC tumors after treatment as shown in Fig. 5a. The results are presented in Fig. 5b. We saw a significant decrease in MDSCs with Nano GMP-ppp dsRNA LCP combination therapy over Nano GMP monotherapy. We also observed a significant increase in T cells and activated DCs only with Nano GMP combination therapy with ppp dsRNA LCP and not with Nano GMP monotherapy. The percentage of T cells increased from $2.99 \pm 0.46\%$ in the PBS group to $5.00 \pm 0.87\%$ in the Nano GMP-ppp dsRNA LCP combination group. Similarly, the proportion of MDSCs in the tumor decreased from $7.52 \pm 1.17\%$ in the Nano GMP monotherapy group to $4.49 \pm 0.25\%$ in the Nano GMP combination therapy arm.

## DISCUSSION

Liposomal nanostructures have been widely explored in small molecule formulation development for gastrointestinal cancers such as pancreatic cancer (29). One of the most prominent and recent success stories in the clinical development of liposomal nanostructures is the approval of Onivyde®, a liposomal formulation of irinotecan in 2015. However, Onivyde® was approved for patients with metastatic pancreatic cancer resistant to gemcitabine. Low cellular uptake and drug resistance limits the efficacy of cytotoxic gemcitabine in desmoplastic tumors like PDAC. In our current study, we formulated gemcitabine monophosphate in an LCP platform capable of distributing to the tumor, thereby bypassing the initial, rate-limiting monophosphorylation in the sequence of serial phosphorylation toward pharmacological activation, and also mitigating the barrier of hydrophilic gemcitabine to penetrate cells crossing the cellular membrane. The LCP nanoparticles, after intravenous administration, were shown to be capable of delivering phosphorylated drug cargo into cancer cells after receptor-mediated endocytosis into endosomes, dissolve at low pH, increase endosomal pressure by osmotic swelling leading to the disruption of endosome and release of entrapped phosphorylated drugs such as nucleic acids, peptides, and small molecules in the cytosol (17). Further, in our previous studies, we demonstrated GMP delivering LCP nanoparticles could arrest mitosis and induce apoptosis in mouse models of non-small cell lung cancer (18).

This study was performed on a tumor model derived from a KPC cell line and engineered to be bioluminescent and fluorescent for quantitative follow-ups. While this derived tumor model resembles the original KPC model, there are some differences in structural organization of this tumor such as loss of glandular structures typically seen in pancreatic cancer, reduction of extracellular matrix, and relatively higher vascularity compared with the classical KPC model (30,31).

When we tested our Nano GMP formulation *in vivo* in the syngeneic orthotopic allograft model of pancreatic cancer using a cell line derived from the KPC model, we found a robust regression in the absolute tumor burden at the sacrifice, 7 days post a single treatment. The tumors in the Nano GMP group were about 50% smaller than tumors in the PBS treated group (Fig. 2a). The free gemcitabine-treated group showed no statistically significant difference with PBS group. This is an encouraging finding as previous studies had shown that while many other subcutaneous and orthotopic models of xenograft and syngeneic pancreatic cancer models in mice are responsive to gemcitabine, KPC model is resistant

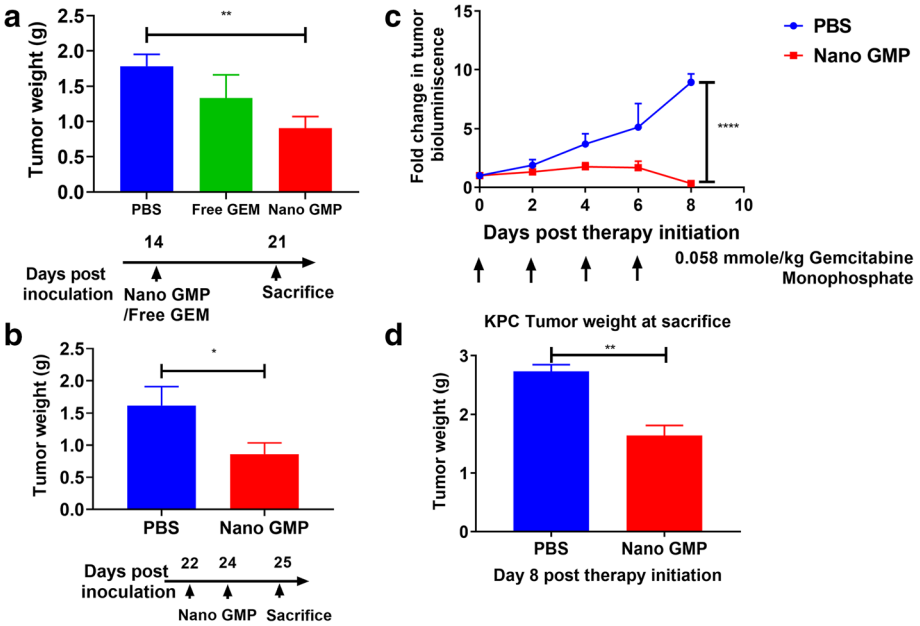


**Fig. 2.** Nanoformulation of Gemcitabine monophosphate enables tumor regression in orthotopic KPC model of pancreatic cancer, **a** pancreatic tumor weight at sacrifice for animals treated with phosphate-buffered saline (PBS), gemcitabine (Free GEM), and gemcitabine monophosphate nanoformulation (Nano GMP). Free GEM or Nano GMP were administered at 0.058 mmole/kg of drug per dose ($n = 4$–5) intravenously on Day 14 and sacrificed on Day 21 post-tumor inoculation, **b** pancreatic tumor weight at sacrifice for a modified treatment regimen ($n = 5$). Nano GMP was administered at 0.058 mmole/kg of drug per dose ($n = 4$–5) intravenously on Day 22 and 24 and sacrificed on Day 25 post-tumor inoculation, **c** treatment with Nano GMP started when mice bearing orthotopic, luciferase expressing KPC tumors reached a radiance of $5 \times 10^7$ per second per centimeter squared per steradian ($n = 3$–4), and therapy was administered four times, every other day, for 6 days after therapy initiation (0.058 mmole/kg of drug per dose). Tumor burden was reported for alternate days, as fold change in radiance, relative to baseline at initiation of the therapy, **d** tumor weights for mice treated following the regimen in 2.c) were reported at sacrifice ($n = 3$–4). Data show mean ± SEM. *$p < 0.05$, **$p < 0.01$, ****$p < 0.0001$

to gemcitabine monotherapy, even at doses of 50–100 mg/kg (31). In our study, we managed to reduce the efficacious dose to 20 mg/kg.

When we modified our treatment regimen to observe the treatment effect on a shorter term, we found a comparable degree of tumor regression as we have seen with the single-treatment regimen above (Fig. 2b). To further determine the cytotoxic effect of the formulated GMP, we monitored the progression of tumor via bioluminescent imaging. We engineered the KPC cells in our study to express firefly luciferase; therefore, the radiant signal served as a proxy for cancer cells in the tumor. The actual proportion of cancer cells in PDAC tumors are low, with fibroblasts and extensive immune infiltrates (22,32,33). When we measured tumor growth via radiance, the apparent difference in tumor burden was even higher, with about 9-fold increase in the PBS group tumors relative to baseline at treatment initiation, *vs.* about 0.33-fold decrease relative to baseline in Nano GMP group (Fig. 2c). The decrease in absolute tumor burden by weight was about 40% for this group, where the untreated tumors had a mean weight of over 2.7 g, more than 10% of the body weight of these animals (Fig. 2d).

In our study, we also observed a significant increase in the percentage of apoptotic cells. Previous studies had shown no significant changes in apoptosis or proliferation of cancer cells in the KPC tumors (31), under gemcitabine treatment. Tissue inhibitor of matrix metalloproteases (TIMP1) is associated with hyperproliferation of $KRAS^{G12D}$ mutant cancer cells and propagates gemcitabine resistance by overexpression in response to treatment, and subsequent perturbation of the processes of proliferation and apoptosis (34). Nano GMP enabled a significant increase in the proportion of apoptotic cells (Fig. 3). It will be worthwhile studying if TIMP1 is still upregulated after treatment with Nano GMP, and if it is comparable with upregulation noted in PDAC tumors after gemcitabine therapy.

Gemcitabine treatment is known to elevate the infiltration of tumor-associated macrophages (TAM) in pancreatic tumors mediated by interleukin (IL)- 8, further promoting cancer stemness, and chemoresistance (35–37). In our study, we saw a decrease in M2 macrophages with Nano GMP, and no significant change in the relative proportion of $CD44^+$ $CD133^+$ cancer stem cells in the tumor, although gemcitabine therapy is associated with increased expression of stem cell-like markers and manifestation of the attributes of epithelial to mesenchymal transition (EMT), following treatment (38). We also saw a significant decrease in the proportion of MDSCs in the KPC tumors with Nano GMP treatment. Inhibition of MDSCs by gemcitabine was not surprising and well documented in previous studies, with both human patients and murine studies (39,40). However, direct comparison of Nano GMP with carrier-free gemcitabine must be

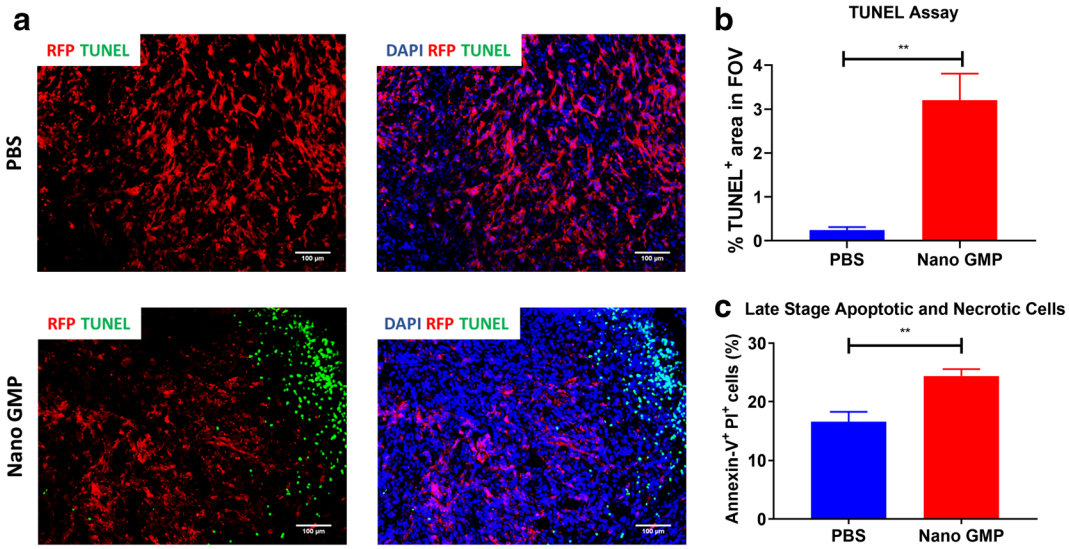


**Fig. 3.** Nanoparticle-mediated delivery of gemcitabine monophosphate enhances apoptosis in pancreatic tumor, **a** terminal deoxynucleotidyl transferase dUTP nick end labeling (TUNEL) assay was used to detect apoptotic DNA fragmentation by immunofluorescence, in fixed paraffin-embedded pancreatic tumor tissue section. Tumor-bearing animals prior to sacrifice were treated with phosphate-buffer saline (PBS) or nanoformulation of gemcitabine monophosphate (Nano GMP), as shown in the treatment regimen in Fig. 2c. Red shows red fluorescent protein (RFP) expressing cancer cells, green shows TUNEL stain-3′-hydroxyl termini of DNA double strand breaks, DAPI is used for blue fluorescent DNA stain, **b** Quantification of the TUNEL staining, as shown in Fig. 3a, by ImageJ. Columns represent the percentage of TUNEL positive staining in microscopic field of view ($n = 3$–4), **c** Annexin V and propidium iodide (PI) double positive cells were identified from total populations of pancreatic tumor cells by flow cytometry ($n = 4$) and presented. Data show mean ± SEM. $^{**}p < 0.01$

conducted in the future for downstream analyses such as flow cytometry studies, to further validate the impact of Nano GMP in modulating the TME in this KPC cell line-derived model.

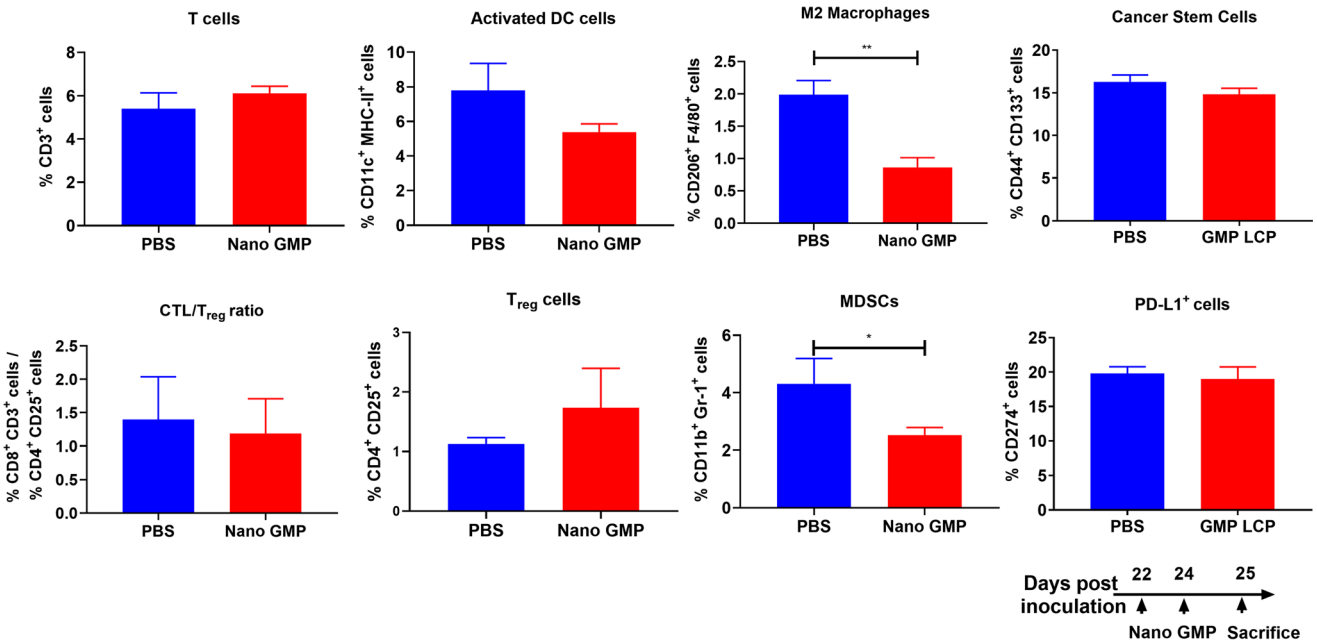


**Fig. 4.** Effect of gemcitabine monophosphate nanoformulation on the cellular composition of the tumor microenvironment. Orthotopic KPC tumor-bearing animals were sacrificed at end of treatment with gemcitabine monophosphate nanoformulation (Nano GMP), as shown in the regimen, Nano GMP was administered at 0.058 mmole/kg of drug per dose intravenously on Day 22 and 24 and sacrificed on Day 25 post-tumor inoculation, and tumor cells from animals were stained by flow cytometry ($n = 4$–5). The results were analyzed by FlowJo and presented. Data show mean ± SEM. $^{*}p < 0.05$. The following markers were used to identify the corresponding cell populations: T cells – $CD3^+$, Activated DCs- $CD11c^+$ $MHC\text{-}II^+$, M2 Macrophages- $CD206^+$ $F4/80^+$, Cancer Stem Cells- $CD44^+$ $CD133^+$, $CTL/T_{reg}$ – $(CD8^+\ CD3^+)/(CD4^+\ CD25^+)$, $T_{reg}$- $CD4^+$ $CD25^+$, MDSCs- $CD11b^+$ $Gr\text{-}1^+$, and PD-L1 cells- $CD274^+$ cells

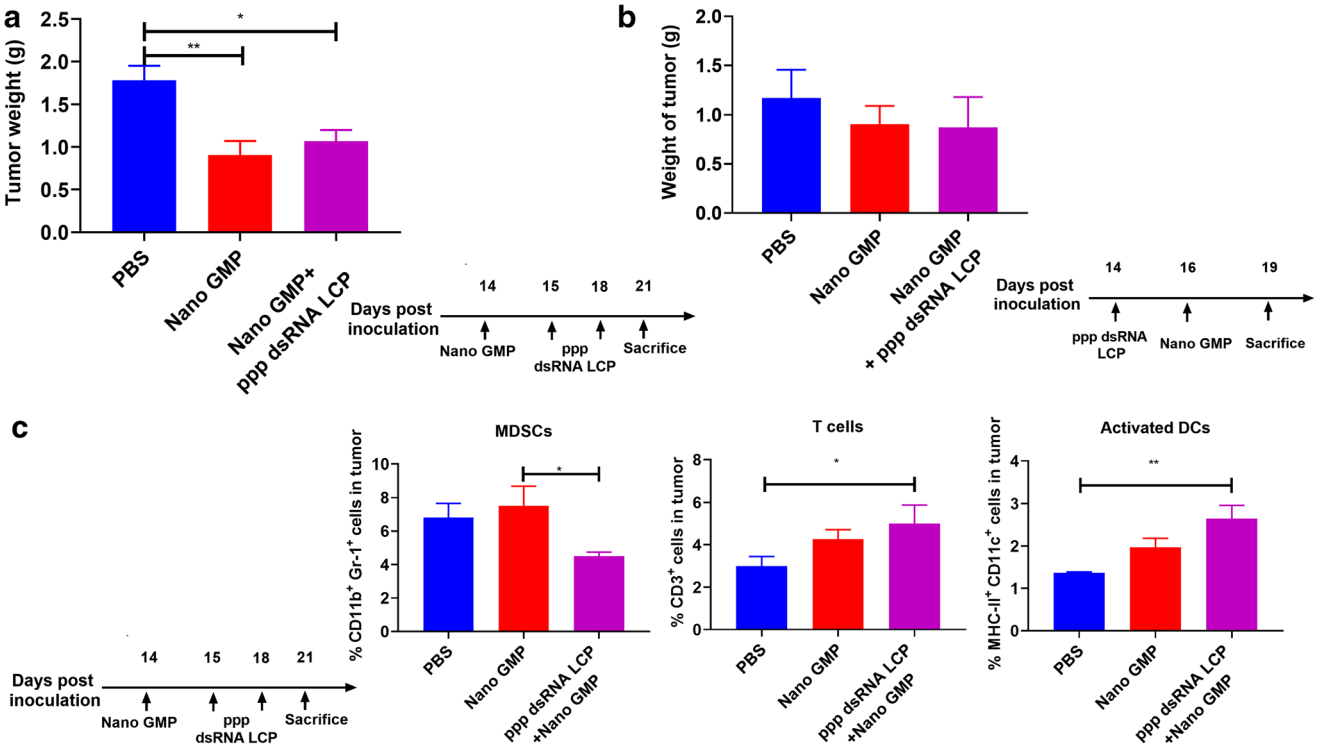


**Fig. 5.** Combination of gemcitabine monophosphate nanoformulation chemotherapy and adjuvant immune therapy can reprogram tumor immune microenvironment, **a** orthotopic KPC tumor-bearing animals were treated with gemcitabine monophosphate nanoformulation (Nano GMP), or a combination of Nano GMP and RIG-I agonist 5′-triphosphate double-stranded RNA (ppp dsRNA LCP), and tumor burden was measured at sacrifice ($n = 4–5$). Nano GMP was administered at 0.058 mmole/kg of drug per dose ($n = 4–5$) intravenously on Day 14, ppp dsRNA was administered at 0.02 μmole/kg of drug per dose intravenously on Day 15 and 18, and mice were sacrificed on Day 21 post-tumor inoculation, **b** tumor burden at sacrifice for a combination therapy of Nano GMP and ppp dsRNA LCP, under a modified dosing schedule ($n = 3–5$). ppp dsRNA was administered at 0.02 μmole/kg of drug per dose intravenously on Day 14, Nano GMP was administered at 0.058 mmole/kg of drug per dose ($n = 4–5$) intravenously on Day 16, and mice were sacrificed on Day 21 post-tumor inoculation, **c** tumor-bearing animals were sacrificed at end of treatment with Nano GMP, or Nano GMP and ppp dsRNA LCP, in a regimen as described in Fig. 5a), and tumor cells from animals were stained by flow cytometry ($n = 4$). The results were analyzed by FlowJo and presented. Data show mean ± SEM. $*p < 0.05$, $**p < 0.01$. The following markers were used to identify the corresponding cell populations: T cells – $CD3^+$, Activated DCs- $CD11c^+$ $MHC\text{-}II^+$, and MDSCs- $CD11b^+$ $Gr\text{-}1^+$ cells

Finally, we combined Nano GMP and retinoic acid-inducible gene I (RIG-I)-agonist ppp dsRNA in a combinatorial therapeutic regimen. We saw a sequence dependence in tumor regression relative to untreated tumors; a significant reduction was only observed when Nano GMP treatment preceded treatment with ppp dsRNA LCP. However, combination therapy with ppp dsRNA did not manifest a significantly improved tumor regression over Nano GMP monotherapy and showed comparable levels of tumor burden, 40–50% lower than PBS treated control tumors (Fig. 5a–b). When we assayed the changes in tumor-infiltrates, we saw an increase in T cells, activated DCs, and a reduction in the MDSCs in the combination therapy arm, unlike the control PBS treated tumors. These observations suggest the combination of immune adjuvant with chemotherapy delivered via LCP nanoparticles could alter the TME; however, the perturbed immune microenvironment did not translate into a synergistic antitumor response. We hypothesize that this lack of translation of immunomodulation to synergistic tumor regression is due to antigen-poor character of KPC tumors. Evans *et al.* had shown KPC tumors progress spontaneously, in presence or absence of T cells, and expresses no neoepitopes that are predicted to bind strongly to major histocompatibility complex class-I molecules, suggesting its immunological cold character, similar to clinical PDAC tumors (41). In the absence of neoantigens to target, it would be unreasonable to expect that an increase in T cell infiltration, and activation of dendritic cells could promote antigen-specific immune response and enhance antitumor activity. The lack of immunogenic antigens will potentially be a barrier in actuating enhanced immunogenic cell death as exploited in other studies by triggering the release of danger-associated molecular patterns (42).

However, there is room for improvement in the therapeutic efficacy. Monophosphorylated gemcitabine can still be vulnerable to deactivation by deoxycytidylate deaminase, which may reduce efficacy. In the future, it will be worthwhile to explore combinatorial strategies to augment the sensitivity of cancer cells to our therapeutic strategy, including re-educating stellate cells and reduction of cancer-associated fibroblasts to further improve nanoparticle penetration in desmoplastic KPC tumors (43,44), silencing of transcription factors such as high mobility group A1 (HMGA1) or hypoxia-inducible factor 1α (HIF1α) and inhibiting the upregulation of oncoproteins such as ERK1/2- factors that are critical in gemcitabine chemoresistance, or co-delivering siRNAs

inhibiting ribonucleotide reductase subunit 2 (RRM2) which reduce the chemosensitivity of gemcitabine (45–49), among others.

We should acknowledge that while we compared free gemcitabine in one of our key *in vivo* tumor regression experiments with Nano GMP herein, and we had thoroughly evaluated the superiority of Nano GMP over free gemcitabine in a mouse model of non-small cell lung cancer (NSCLC) previously (19), we have not compared Nano GMP with free gemcitabine in many other *in vivo* and ex vivo tumor characterization experiments in the current study. Larger sample sizes, consistent inclusion of free gemcitabine as a control, and follow-up of tumor growth through long-term survival studies can help further evaluate the efficacy of Nano GMP in this desmoplastic KPC model of pancreatic cancer.

Lastly, we acknowledge that there are limitations in translating the current LCP nanoparticles for clinical application, due to pharmacokinetic properties such as short half-life, biodistribution to RES organs, and scalability challenges such as harsh physical resuspension processes. However, we have also shown that these challenges can be bypassed for liposomal nanoparticles such as LCP by redesigning the outer leaflet lipids to solely incorporate PEGylated phospholipids, varying the PEG chain lengths to extend circulation and tune biodistribution and finally allowing resuspension of formulation from lipid films without requirement of disruptive, high-energy methods (50).

## CONCLUSION

In summary, we showed that nanoformulation of GMP could induce a robust antitumor response and trigger apoptosis in a desmoplastic, clinically relevant KPC cell line-derived model of pancreatic cancer. Further, Nano GMP did not result in infiltration of immunosuppressive cells such as tumor-associated macrophages and rather led to reduction of immunosuppressive macrophage and MDSC populations. We also did not see any significant increase in the proportion of cancer stem cells, although gemcitabine treatment is associated with the increase in expression of cancer stem cell-like markers. Therefore, nanoformulation of GMP, a metabolite of gemcitabine, enabled robust tumor regression in an aggressive PDAC model with a low parenteral dose and circumvented some of the major hallmarks of chemoresistance commonly seen after gemcitabine treatment. However, for probable reasons we discussed above, this nano-therapy was not found to be suitable for combination therapy aimed at augmenting the efficacy of immunotherapy.

## FUNDING INFORMATION

The work was supported by National Institute of Health (NIH) grant CA198999, from National Cancer Institute (NCI).

## COMPLIANCE WITH ETHICAL STANDARDS

**Conflict of Interest** L.H. is a consultant for PDS Biotechnology, Samyang Biopharmaceutical, Stemirna, and Beijing Inno Medicine.

**Human and animal rights and informed consent** All animal experiments were conducted in compliance with regulations of the University of North Carolina at Chapel Hill Institutional Animal Care and Use Committee (IACUC).

## REFERENCES

1. Howlader NNA, Krapcho M, Miller D, Brest A, Yu M, Ruhl J, et al. (eds). SEER Cancer Statistics Review. National Cancer Institute Bethesda, MD, https://seer.cancer.gov/csr/1975_2016/, based on November 2018 SEER data submission 1975–2016.
2. Hidalgo M. Pancreatic cancer. N Engl J Med. 2010;362(17):1605–17.
3. Zhang H. Onivyde for the therapy of multiple solid tumors. Onco Targets Ther. 2016;9:3001–7.
4. Buscail L, Bournet B, Cordelier P. Role of oncogenic KRAS in the diagnosis, prognosis and treatment of pancreatic cancer. Nat Rev Gastroenterol Hepatol. 2020;17:153–68.
5. Jordheim LP, Durantel D, Zoulim F, Dumontet C. Advances in the development of nucleoside and nucleotide analogues for cancer and viral diseases. Nat Rev Drug Discov. 2013;12(6):447–64.
6. de Sousa Cavalcante L, Monteiro G. Gemcitabine: metabolism and molecular mechanisms of action, sensitivity and chemoresistance in pancreatic cancer. Eur J Pharmacol. 2014;741:8–16.
7. Senanayake TH, Warren G, Vinogradov SV. Novel anticancer polymeric conjugates of activated nucleoside analogues. Bioconjug Chem. 2011;22(10):1983–93.
8. Karasek P, Skacel T, Kocakova I, Bednarik O, Petruzelka L, Melichar B, et al. Gemcitabine monotherapy in patients with locally advanced or metastatic pancreatic cancer: a prospective observational study. Expert Opin Pharmacother. 2003;4(4):581–6.
9. Oguri T, Achiwa H, Sato S, Bessho Y, Takano Y, Miyazaki M, et al. The determinants of sensitivity and acquired resistance to gemcitabine differ in non-small cell lung cancer: a role of ABCC5 in gemcitabine sensitivity. Mol Cancer Ther. 2006;5(7):1800–6.
10. Benjamin RS. Rationale for the use of mitoxantrone in the older patient: cardiac toxicity. Semin Oncol. 1995;22(1 Suppl 1):11–3.
11. Huang P, Chubb S, Hertel LW, Grindey GB, Plunkett W. Action of 2′,2′-difluorodeoxycytidine on DNA synthesis. Cancer Res. 1991;51(22):6110–7.
12. Heinemann V, Xu YZ, Chubb S, Sen A, Hertel LW, Grindey GB, et al. Cellular elimination of 2′,2′-difluorodeoxycytidine 5′-triphosphate: a mechanism of self-potentiation. Cancer Res. 1992;52(3):533–9.
13. Allain V, Bourgaux C, Couvreur P. Self-assembled nucleolipids: from supramolecular structure to soft nucleic acid and drug delivery devices. Nucleic Acids Res. 2012;40(5):1891–903.
14. Rejiba S, Reddy LH, Bigand C, Parmentier C, Couvreur P, Hajri A. Squalenoyl gemcitabine nanomedicine overcomes the low efficacy of gemcitabine therapy in pancreatic cancer. Nanomedicine. 2011;7(6):841–9.
15. Du C, Qi Y, Zhang Y, Wang Y, Zhao X, Min H, et al. Epidermal growth factor receptor-targeting peptide nanoparticles simultaneously deliver gemcitabine and olaparib to treat pancreatic cancer with breast cancer 2 ( BRCA2) mutation. ACS Nano. 2018;12(11):10785–96.
16. Li F, Zhao X, Wang H, Zhao R, Ji T, Ren H, et al. Multiple layer-by-layer lipid-polymer hybrid nanoparticles for improved FOLFIRINOX chemotherapy in pancreatic tumor models. Adv Funct Mater. 2015;25(5):788–98.
17. Li J, Chen YC, Tseng YC, Mozumdar S, Huang L. Biodegradable calcium phosphate nanoparticle with lipid coating for systemic siRNA delivery. J Control Release. 2010;142(3):416–21.

18. Zhang Y, Schwerbrock NM, Rogers AB, Kim WY, Huang L. Codelivery of VEGF siRNA and gemcitabine monophosphate in a single nanoparticle formulation for effective treatment of NSCLC. Mol Ther. 2013;21(8):1559–69.
19. Zhang Y, Kim WY, Huang L. Systemic delivery of gemcitabine triphosphate via LCP nanoparticles for NSCLC and pancreatic cancer therapy. Biomaterials. 2013;34(13):3447–58.
20. Zhang J, Miao L, Guo S, Zhang Y, Zhang L, Satterlee A, et al. Synergistic anti-tumor effects of combined gemcitabine and cisplatin nanoparticles in a stroma-rich bladder carcinoma model. J Control Release. 2014;182:90–6.
21. Zhang Y, Peng L, Mumper RJ, Huang L. Combinational delivery of c-myc siRNA and nucleoside analogs in a single, synthetic nanocarrier for targeted cancer therapy. Biomaterials. 2013;34(33):8459–68.
22. Das M, Shen L, Liu Q, Goodwin TJ, Huang L. Nanoparticle delivery of RIG-I agonist enables effective and safe adjuvant therapy in pancreatic cancer. Mol Ther. 2019;27(3):507–17.
23. Satterlee AB, Huang L. Current and future theranostic applications of the lipid-calcium-phosphate nanoparticle platform. Theranostics. 2016;6(7):918–29.
24. Westphalen CB, Olive KP. Genetically engineered mouse models of pancreatic cancer. Cancer J. 2012;18(6):502–10.
25. Clark CE, Beatty GL, Vonderheide RH. Immunosurveillance of pancreatic adenocarcinoma: insights from genetically engineered mouse models of cancer. Cancer Lett. 2009;279(1):1–7.
26. Clark CE, Hingorani SR, Mick R, Combs C, Tuveson DA, Vonderheide RH. Dynamics of the immune reaction to pancreatic cancer from inception to invasion. Cancer Res. 2007;67(19):9518–27.
27. Zheng L. Immune defects in pancreatic cancer. Ann Pancreat Cancer. 2018;1.
28. Liu Q, Zhu H, Liu Y, Musetti S, Huang L. BRAF peptide vaccine facilitates therapy of murine BRAF-mutant melanoma. Cancer Immunol Immunother. 2018;67(2):299–310.
29. Das M, Huang L. Liposomal nanostructures for drug delivery in gastrointestinal cancers. J Pharmacol Exp Ther. 2019;370(3):647–56.
30. Miao L, Li J, Liu Q, Feng R, Das M, Lin CM, et al. Transient and local expression of chemokine and immune checkpoint traps to treat pancreatic cancer. ACS Nano. 2017;11(9):8690–706.
31. Olive KP, Jacobetz MA, Davidson CJ, Gopinathan A, McIntyre D, Honess D, et al. Inhibition of hedgehog signaling enhances delivery of chemotherapy in a mouse model of pancreatic cancer. Science. 2009;324(5933):1457–61.
32. Spear S, Candido JB, McDermott JR, Ghirelli C, Maniati E, Beers SA, et al. Discrepancies in the tumor microenvironment of spontaneous and orthotopic murine models of pancreatic cancer uncover a new immunostimulatory phenotype for B cells. Front Immunol. 2019;10:542.
33. Zhu Y, Herndon JM, Sojka DK, Kim KW, Knolhoff BL, Zuo C, et al. Tissue-resident macrophages in pancreatic ductal adenocarcinoma originate from embryonic hematopoiesis and promote tumor progression. Immunity. 2017;47(3):597.
34. D'Costa Z, Jones K, Azad A, van Stiphout R, Lim SY, Gomes AL, et al. Gemcitabine-induced TIMP1 attenuates therapy response and promotes tumor growth and liver metastasis in pancreatic cancer. Cancer Res. 2017;77(21):5952–62.
35. Deshmukh SK, Tyagi N, Khan MA, Srivastava SK, Al-Ghadhban A, Dugger K, et al. Gemcitabine treatment promotes immunosuppressive microenvironment in pancreatic tumors by supporting the infiltration, growth, and polarization of macrophages. Sci Rep. 2018;8(1):12000.
36. Mitchem JB, Brennan DJ, Knolhoff BL, Belt BA, Zhu Y, Sanford DE, et al. Targeting tumor-infiltrating macrophages decreases tumor-initiating cells, relieves immunosuppression, and improves chemotherapeutic responses. Cancer Res. 2013;73(3):1128–41.
37. Weizman N, Krelin Y, Shabtay-Orbach A, Amit M, Binenbaum Y, Wong RJ, et al. Macrophages mediate gemcitabine resistance of pancreatic adenocarcinoma by upregulating cytidine deaminase. Oncogene. 2014;33(29):3812–9.
38. Kim MP, Shah AN, Parikh NU, Gallick GE. Gemcitabine resistance in pancreatic cancer cells is associated with increased expression of stem cell-like markers and a concomitant down-regulation of PTEN and activation of AKT. Pancreas. 2007;35(4):409.
39. Le HK, Graham L, Cha E, Morales JK, Manjili MH, Bear HD. Gemcitabine directly inhibits myeloid derived suppressor cells in BALB/c mice bearing 4T1 mammary carcinoma and augments expansion of T cells from tumor-bearing mice. Int Immunopharmacol. 2009;9(7–8):900–9.
40. Wang Z, Till B, Gao Q. Chemotherapeutic agent-mediated elimination of myeloid-derived suppressor cells. Oncoimmunology. 2017;6(7):e1331807.
41. Evans RA, Diamond MS, Rech AJ, Chao T, Richardson MW, Lin JH, et al. Lack of immunoediting in murine pancreatic cancer reversed with neoantigen. JCI Insight. 2016;1(14).
42. Zhao X, Yang K, Zhao R, Ji T, Wang X, Yang X, et al. Inducing enhanced immunogenic cell death with nanocarrier-based drug delivery systems for pancreatic cancer therapy. Biomaterials. 2016;102:187–97.
43. Hu K, Miao L, Goodwin TJ, Li J, Liu Q, Huang L. Quercetin remodels the tumor microenvironment to improve the permeation, retention, and antitumor effects of nanoparticles. ACS Nano. 2017;11(5):4916–25.
44. Han X, Li Y, Xu Y, Zhao X, Zhang Y, Yang X, et al. Reversal of pancreatic desmoplasia by re-educating stellate cells with a tumour microenvironment-activated nanosystem. Nat Commun. 2018;9(1):3390.
45. Kuramitsu Y, Wang Y, Kitagawa T, Tokuda K, Akada J, Tokunaga M, et al. High-mobility group box 1 and mitogen-activated protein kinase activated protein kinase-2 are up-regulated in gemcitabine-resistant pancreatic cancer cells. Anticancer Res. 2015;35(7):3861–5.
46. Zheng C, Jiao X, Jiang Y, Sun S. ERK1/2 activity contributes to gemcitabine resistance in pancreatic cancer cells. J Int Med Res. 2013;41(2):300–6.
47. Wallez Y, Dunlop CR, Johnson TI, Koh SB, Fornari C, Yates JWT, et al. The ATR inhibitor AZD6738 synergizes with gemcitabine in vitro and in vivo to induce pancreatic ductal adenocarcinoma regression. Mol Cancer Ther. 2018;17(8):1670–82.
48. Zhao X, Wang X, Sun W, Cheng K, Qin H, Han X, et al. Precision design of nanomedicines to restore gemcitabine chemosensitivity for personalized pancreatic ductal adenocarcinoma treatment. Biomaterials. 2018;158:44–55.
49. Zhao X, Li F, Li Y, Wang H, Ren H, Chen J, et al. Co-delivery of HIF1alpha siRNA and gemcitabine via biocompatible lipid-polymer hybrid nanoparticles for effective treatment of pancreatic cancer. Biomaterials. 2015;46:13–25.
50. Haynes MT, Huang L. Maximizing the supported bilayer phenomenon: liposomes comprised exclusively of PEGylated phospholipids for enhanced systemic and lymphatic delivery. ACS Appl Mater Interfaces. 2016;8(37):24361–7.